

Received: 2014.05.28
Accepted: 2014.07.04
Published: 2014.10.02

Diffusion Tensor Imaging of Spinocerebellar Ataxia Type 12

Authors' Contribution:
Study Design A
Data Collection B
Statistical Analysis C
Data Interpretation D
Manuscript Preparation E
Literature Search F
Funds Collection G

ABCE **Haitao Li**
CD **Jingjing Ma**
AFG **Xiaoning Zhang**

Department of Neurology, First Affiliated Hospital, Xinjiang Medical University, Urumqi, China

Corresponding Author: Haitao Li, e-mail: 1641241599@qq.com
Source of support: Grants from the Autonomous Region Nature Foundation 2011211A063

Background: Spinocerebellar ataxias (SCAs) are autosomal-dominant neurodegenerative diseases that are clinically and genetically heterogeneous. SCAs are characterized by a range of neurological symptoms. SCA12 is an autosomal-dominant (AD) ataxia caused by a CAG repeat expansion mutation in a presumed promoter region of the gene PPP2R2B in a non-coding region on chromosome 5q32. This study sought to determine changes in different positions in a single Uyghur SCA12 pedigree by measuring the apparent diffusion coefficient (ADC) and fractional anisotropy (FA).





Material/Methods: A single Uyghur pedigree was collected and was confirmed to possess SCA12 by genetic diagnosis, among which 13 cases were patients and 54 cases were "healthy" individuals. Five patients were presymptomatic and 15 individuals selected as a control group were examination in the same time. DTI was performed on a 1.5T scanner, with $b=1000$ s/mm² and 15 directions. ADC and FA were measured by regions of interest positioned in the corticospinal tract at the level of the pons (pons), superior peduncle (SCP), middle cerebellar peduncle (MCP), cerebellar cortex (CeC), cerebral cortex (CC), and cerebellar vermis (CV) white matter.

Results: Compared with the controls, the ADC was significantly elevated in the CeC, SCP, CC, and CV regions in SCA12 patients. The FA significantly decreased in the CC region in SCA12 patients and the CC and CV regions in SCA12 presymptomatic patients. The course of the disease, SARA score, and ADC values in CV showed highly positive correlations.

Conclusions: SCA12 pedigree patients exhibited microstructural damage in the brain white matter. The damage in white matter fiber may first occur in the CC and CV regions in SCA12 presymptomatic patients. The ADC values in the CV region could reflect disease severity in SCA12 patients.

MeSH Keywords: **Anisotropy • Diffusion Tensor Imaging • Spinocerebellar Ataxias**

Full-text PDF: <http://www.medscimonit.com/abstract/index/idArt/891104>

 2673  3  3  28



Background

Spinocerebellar ataxias (SCAs) are autosomal-dominant neurodegenerative diseases that are clinically and genetically heterogeneous. SCAs are characterized by a range of neurological symptoms, including loss of balance and motor coordination, which are caused by progressive dysfunction of the cerebellum and its afferent and efferent connections. Clinical diagnosis of specific subtypes is difficult because of the overlap of phenotypes among genetic subtypes and the variability in clinical features found within distinct genetic subtypes. SCA12 is an autosomal-dominant (AD) ataxia caused by a CAG repeat expansion mutation in a presumed promoter region of the gene PPP2R2B in a non-coding region on chromosome 5q32. Srivastava et al. [1] determined that SCA12 is very rare, accounting for only 6.5% of all AD cases. Pathogenesis is likely caused by repetition, amplification, and mutation of CAG, which can affect the transcription of the promoter. The structure of 1 shear transcription of PPP2R2B or other types of genetic expression can change the conformation and functions of the adjusting subunit of protein phosphatase 2A to strengthen chondriokinesis, thereby resulting in neuronal pathology. An action tremor is a prominent feature in SCA12, and is often the presenting neurologic sign. Action tremors then gradually develop into ataxia gait, head tremor, hypokinesia, abnormal eye movements, and tendon hyperreflexia; in patients with dementia, mood disorders may occur [2–6].

Atrophy of both the cerebral cortex and cerebellum has been reported on either computed tomography (CT) or brain magnetic resonance imaging (MRI) images from SCA12 patients in a North American kindred and Indian SCA12 patients. Generalized cerebral cortical atrophy is accompanied by moderate ventriculomegaly. Basal ganglia and brainstem structures are relatively preserved. The vermis of the cerebellum appears more atrophic than the cerebellar hemispheres. No focal signal abnormalities in grey or white matter have been reported in SCA12 brain images [6].

Neuropathology of the SCA12 proband revealed atrophy of the cerebral cortex and cerebellum plus mild pontine atrophy. Microscopic examination of this SCA12 brain demonstrated moderate-to-marked Purkinje cell loss and atrophy of the cerebellar granule cell layer. Neuronal intranuclear inclusions were found in dopamine neurons of the substantia nigra, Purkinje cells, and rare motor cortical neurons.

Diffusion tensor imaging (DTI) refers to the use of water molecule diffusion anisotropy of nerve fibers in multiple directions on a diffusion-sensitive gradient. DTI detects each individual element of water molecular diffusion anisotropy, and reflects the fine structure of cerebral white matter fiber tracts of damage through the obtained fractional anisotropy (FA) and apparent diffusion coefficient (ADC) values. DTI provides a non-invasive

method of showing living brain white matter nerve fiber access, reflects the diffusion of water molecules, and provides a quantitative description of organization by diffuse anisotropy. DTI has potential for broad clinical application. ADC mainly reflects the diffusion speed of water molecules without indicating the direction of movement. When nerve degeneration occurs, nerve cell loss and myelin depigmentation increase the movement of water molecules. Therefore, the rate of diffusion of water molecules increases, and anisotropy decreases. The FA value can reflect the consistency of nerve fibers, structural tightness, and integrity of microstructure. ADC and FA values obtained from DTI have gained widespread acceptance as sensitive indicators to quantify microstructural damage of gray and white matter in neurodegenerative diseases. ADC and FA values have recently been used in the study of SCAs. The evaluation of deep cerebellar nuclei (DCN) using DTI can serve as a simple imaging biomarker of cerebellar disease.

As of this writing, reports on SCA12 using DTI analysis are rare. In this study, changes in ADC and FA in SCA12 were investigated to determine whether they cause damage to white matter. Significant correlations of ADC and FA with disease course and clinical scores were also determined. By detecting different types of micro-damage in brain white matter structure in the presymptomatic patients and a control group of a large Uighur SCA12 pedigree using DTI, morphological markers were found to have an important function in early judgment of the morbidity situation of presymptomatic patients and the quantitative assessment of the severity of disease in patients.

Material and Methods

Data

Participants were Uyghur patients and their family members preliminarily diagnosed with SCA based on the Harding standard. Data from 1 Uyghur pedigree were collected, among which 13 cases were patients and 54 cases are “healthy” individuals from Xinjiang. The study used the tracking investigation method and selected 1 Uyghur pedigree using the following criteria: (1) with pedigree analysis, the genetic mode of the disease in the family are autosomal-dominant inheritance; (2) chronic progressive disorder of cerebellar ataxia was the main clinical manifestation; (3) imaging changes in the cerebellum and brainstem atrophy as the main features.

Exclusion criteria: Other diseases that can cause cerebellar ataxia, like multiple sclerosis, cerebellar tumor, inflammation, and cerebral vascular diseases.

The diagnosis was genetically confirmed by means of polymerase chain reaction (PCR) of the gene expansions, agarose

Table 1. The clinical characteristics and SARA rating for 13 cases with SCA12.

Patient No.	IV-1	III-5	IV-7	III-8	III-10	III-18	IV-2	IV-4	IV-9	IV-21	IV-11	IV-14	IV-16
Gender	Female	Male	Female	Male	Female	Male	Male	Male	Male	Male	Female	Female	Female
Age at present	48	61	47	54	59	55	42	41	41	44	38	48	43
Onset age	44	53	42	53	48	40	40	39	33	42	36	41	40
Course of disease	4	8	5	1	11	15	7	2	8	2	2	7	3
CAG Repetition times	48	50	52	51	50	54	49	49	48	50	52	50	50
Unstable walking	-	Serious	+	+	+	Serious	-	+	+	+	+	Serious	-
Alalia	-	Obvious	+	+	+	Obvious	-	-	+	+	+	+	-
Tremble in upper limbs	Mild	Obvious	Moderate	Moderate	Without	Obvious	Mild	Moderate	Moderate	Moderate	-	Obvious	Mild
Dysphagia	-	+	-	-	-	With	-	-	-	-	-	+	-
Diminution of vision	-	+	-	-	-	-	-	-	-	-	-	-	-
Nystagmus and slow eye movement	-	Obvious	+	-	-	-	-	-	+	-	+	Obvious	-
Orthostatic dizziness	-	Obvious	+	+	+	Obvious	-	-	+	+	+	Obvious	-
Amyotrophy	-	-	-	-	-	-	-	-	-	-	-	-	-
Muscular tension	Normal	Enhanced	Normal	Normal	Normal	Active	Normal	Enhanced	Normal	Normal	Normal	Active	Healthy
Tendon reflex	Enhanced	Active	Enhanced	Enhanced	Enhanced	Active	Normal	Active	Enhanced	Active	Enhanced	Active	Healthy
Pathological reflex	Negative	Positive	Positive	Positive	Positive	Positive	Negative	-	Positive	Negative	Positive	Positive	Negative
Sensory disturbance	-	+	-	-	-	-	-	+	-	-	-	-	-
Intelligence declining	-	+	-	-	+	+	-	+	-	-	+	+	-
SARA grade (marks)	9	28	25	12	32	35	5	19	15	12	23	28	11

CAG – indicates cytosine adenine guanine.

gel electrophoresis, and T carrier molecular cloning technology, to be combined with digestion identification and other techniques as described elsewhere. The genetics-based diagnosis of SCA12 patients, including 7 male patients and 6 female patients, with average disease onset age of 43.00 ± 6.56 years old and the mean course of the disease was (6.92 ± 4.82) years. In 5 presymptomatic patients (2 male, 3 female), average age at disease onset was (31.12 ± 2.56) years old. The control group included 15 healthy Uyghur individuals without blood relationship and with average age of 35.65 ± 3.75 years. Five presymptomatic patients with SCA12 and 13 other patients were scanned as part of a locally approved multicenter study. We obtained

written informed consent from all participants, in accordance with institutional guidelines and with the Helsinki declaration.

The clinical characteristics of the patients are given in Table 1 and 2. We also enrolled 3.15 age-matched controls (7 male and 8 female, age 38.36 ± 3.46 years) without a history of neurologic disturbances, with normal results on brain MR imaging, who did not smoke, drink, or take medications that act on the CNS.

The protocol of the study was approved by the medical Ethics Committee of the First Affiliated Hospital of Xinjiang Medical University (Approval No. 20090822007).

Table 2. Encephalatrophy grading in different position.

Patient No.	Duration of disease	Encephalatrophy grading							
		Frontal lobe	Parietal lobe	Temporal lobe	Occipital lobe	Midbrain	Pons	Medulla oblongata	Cerebellum
SCA12-1	15	2	2	0	0	1	3	1	3
SCA12-2	11	1	1	0	1	1	2	3	3
SCA12-3	8	1	1	0	0	0	1	0	2
SCA12-4	8	1	0	0	0	0	1	0	1
SCA12-5	7	1	1	0	0	0	0	0	1
SCA12-6	7	1	0	0	0	0	0	0	1
SCA12-7	5	1	0	0	0	0	0	0	0
SCA12-8	4	1	0	0	0	0	0	0	1
SCA12-9	3	0	0	0	0	0	0	0	0
SCA12-10	2	0	0	0	0	0	0	0	0
SCA12-11	2	0	0	0	0	0	0	0	0
SCA12-12	2	0	0	0	0	0	0	0	0
SCA12-13	1	0	0	0	0	0	0	0	0

MRI

On the day of scanning, patients were assessed by a senior neurologist using the Scale for the Assessment and Rating of Ataxia (SARA), which quantifies the degree of neurologic impairment, with scores ranging from 0 (no ataxia) to 40 (most severe ataxia) (Table 1).

We used an Achieva 1.5T double-gradient magnetic resonance scanner (Philips) and an 8-channel head coil SENSE. The scanning methods employed included conventional scan and DTI scan. The conventional scanning line used the conventional spin-echo sequences for T1WI and T2WI. DTI cross-sectional scan levels were consistent with conventional MRI, and diffusion-weighted single-excitation SE-EPI sequences were used.

DTI

DTI was performed with a twice-refocused, single-shot, spin-echo echo-planar sequence, using 15 directions and $b=1000$ s/mm². The following conditions were used in DTI: TR, 2644 ms; TE, 55.0 ms; NEX, 1; 256×256 matrix; FOV, 230×230 mm; thickness, 6.0 mm; and no intersection gap.

Original data were collected in a post-processing workstation and a post-processing “dispersion” software package was used to establish the ADC and FA values. Transverse bitmap T1WI and T2WI were used as a reference, and placed in regions of interest (ROIs). The approximate ROI was selected in the contralateral corresponding parts. The ROI size was about 7 mm.

To increase accuracy, a high-definition positioning FLAIR figure was selected. A FLAIR map matching positioning was then employed to outline the ROI area in the bilaterally symmetric cerebral hemisphere. ADC and FA were measured with planar circular ROIs positioned on the DTI color maps jointly by 2 neuroradiologists blinded to patient identity, clinical data, and structural imaging. The FA and DC values were determined in each ROI, and were subsequently measured 3 times. The data were then averaged. ROI was positioned mainly in the following regions: the corticospinal tract (CST) at the level of the pons (pons), superior peduncle (SCP), middle cerebellar peduncle (MCP), cerebellar cortex (CeC), cerebral cortex (CC), and cerebellar vermis (CV) white matter.

Statistical analysis

Six different positions of the ADC and FA values were measured in 3 groups (patients, presymptomatic patients, and control group). Data were inputted using SPSS19.0 software. A normal distribution of the obtained data was shown using the normality test and distribution curve. Differences among the 3 groups in 6 different positions of the 2 indicators (ADC and FA values) were examined and the Kruskal-Wallis H test was used for the 3 groups and the Wilcoxon test was used for multiple-comparison. For SCA12 patients, multiple linear correlation analysis was used to determine any correlations in the CAG repeat frequency, duration, SARA score, and different position between the ADC and FA values. Data are expressed as mean ± standard deviation. The significance level was set at $P<0.05$.

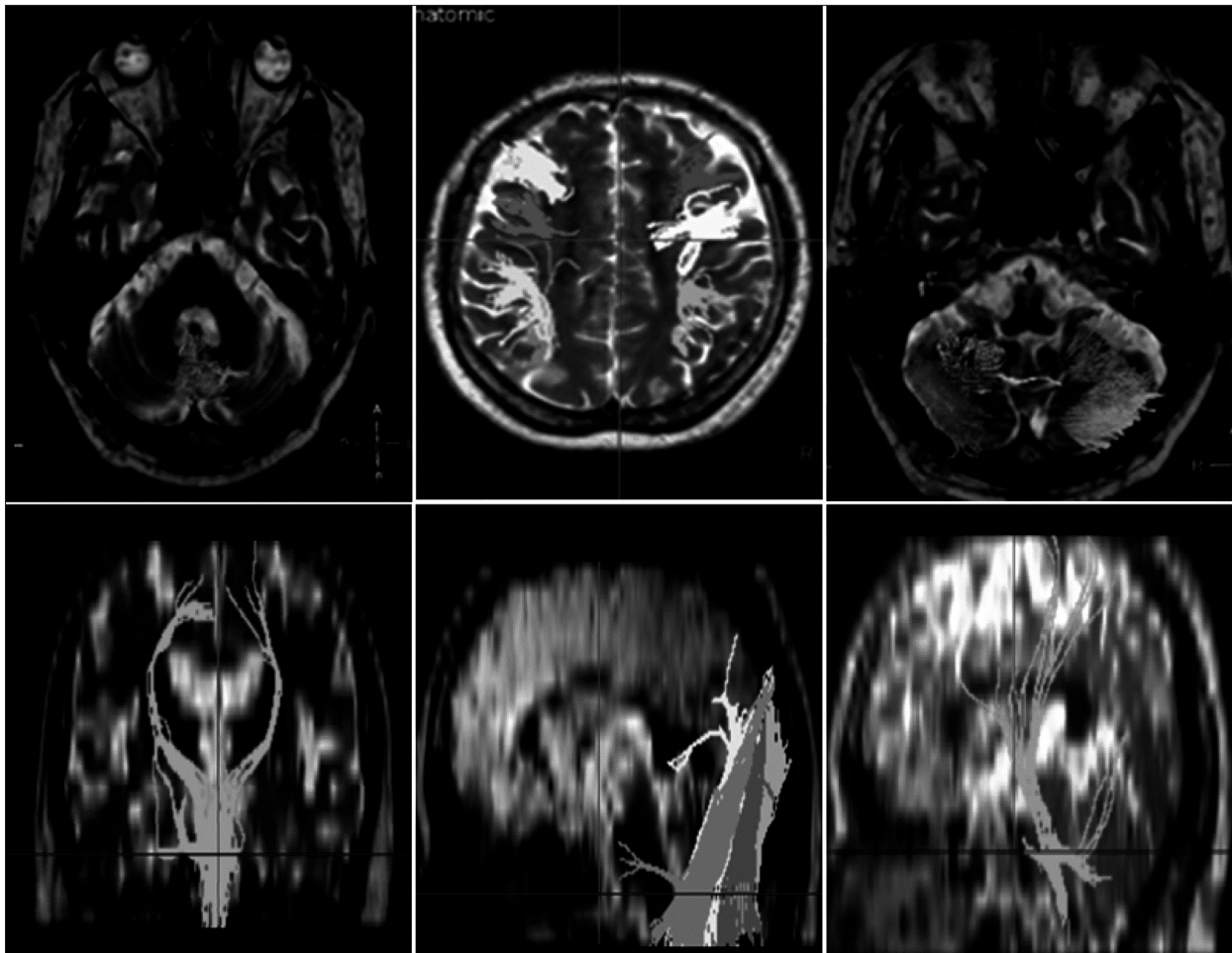


Figure 1. MRI scanning of head for the proband.

Results

MRI

The standard for the evaluation of encephalatrophy degrees is: 0 stands for normal brain structure, 1 is for mild encephalatrophy (deepening anfractuosity and thinning gyrus), 2 is for moderate encephalatrophy (more obvious deepening of anfractuosity, thinning gyrus with obvious shrinking, and mild expansion to the ventricle), and 3 is for serious encephalatrophy (anfractuosity deepening to alba, thinning gyrus with obvious shrinkage, and obvious expansion in the ventricle and cistern) (Table 2).

To summarize the MRI manifestations of patients with SCA12: 9 cases had cerebral cortex shrinkage in the frontal lobe, parietal lobe, and other parts; 12 cases exhibited shrinkage in the CV, overall shrinkage in the cerebellar hemispheres characterized by deepening and widening of anfractuosity in the ependymal cortex and thinning of gyrus; and 7 cases had brainstem atrophy, including volume shrinkage in pons and

medulla, expansion of the pons forebay, and other characteristics (Figure 1).

DTI

The Kruskal-Wallis H test was used in the 3 groups. Based on the different positions of ADC values, no statistically significant difference was found in the positions of the MCP and CST pons among the 3 groups ($P>0.05$). By contrast, the positions in the SCP, CeC, CC, and CV white matter were found to be significantly different among the 3 groups ($P<0.05$). The Wilcoxon test was used for multiple-comparison. The results showed a statistically significant difference in the positions of the SCP, CeC, CC, and CV white matter between the patients and normal group ($P<0.05$). ADC values in the patients were higher than those in the normal group, and the position of CV white matter was significantly different between the patients and presymptomatic patients ($P<0.05$).

The Kruskal-Wallis H test was used in the 3 groups. Based on the different positions of FA values, significant differences in

Table 3. Results from post hoc comparisons for ADC, FA between patients, presymptomatic patients and controls with SCA12, the comparison results between three groups.

	Patients	Pre-	Control	χ^2	P	Patients-control	Pre-control	Patients-pre
ADS								
CeC	0.776±0.075	0.739±0.013	0.740±0.015	13.58	*	*	ns	ns
CV	0.869±0.078	0.800±0.045	0.784±0.040	10.25	**	***	ns	*
CC	0.793±0.048	0.772±0.034	0.753±0.012	18.34	*	**	ns	ns
MCP	0.735±0.042	0.747±0.039	0.741±0.011	6.38	ns	ns	ns	ns
SCP	0.780±0.036	0.774±0.023	0.746±0.020	19.58	**	**	ns	ns
CST (pone)	0.846±0.046	0.890±0.079	0.877±0.022	2.27	ns	ns	ns	ns
PA								
CeC	0.365±0.032	0.370±0.034	0.373±0.007	1.24	ns	ns	ns	ns
CV	0.364±0.036	0.428±0.039	0.357±0.019	27.22	***	ns	***	***
CC	0.333±0.037	0.346±0.010	0.313±0.007	11.68	*	*	*	ns
MCP	0.443±0.037	0.450±0.089	0.435±0.023	1.37	ns	ns	ns	ns
SCP	0.463±0.038	0.412±0.066	0.445±0.026	4.78	ns	ns	ns	*
CST (pone)	0.465±0.027	0.420±0.081	0.452±0.021	6.25	ns	ns	ns	*

CST(pons) – indicates corticospinal tract at the level of the pons; SCP – in the superior peduncle; MCP – middle cerebellar peduncle; CeC – in the Cerebellar Cortex; CC – in the Cerebral Cortex; CV – in the Cerebellar vermis white matter. Pre – indicates Presymptomatic patients. n.s. – not significant. Values are expressed as mean ±SD. * P=.05; ** P=.01; *** P=.001.

the positions of the SCP, CC, and CV were observed among the 3 groups (P<0.05). The Wilcoxon test was used for multiple-comparison. The results show that the position of the CC was significantly different between the patients and normal group (P<0.05). FA values in the patients were lower than those in the normal group. Significant differences in the positions of the CV and CC were observed between the presymptomatic patients and normal group (P<0.05). FA values in the presymptomatic patients were lower than those in the normal group in the CV.

Randomized differential analysis was employed in the 3 groups. The results show that the positions of the CST (pons), SCP, MCP, CeC, CC, and CV white matter were significantly different based on the 2 indicators (ADC and FA values) among the 3 groups (P<0.05).

Correlation analysis showed that the SARA score was correlated with ADC in the CV white matter (r=0.72, P<0.05). Disease duration was correlated with ADC in the CV white matter (r=0.71, P<0.05) (Table 3, Figures 2, 3).

Discussion

DTI revealed disease-specific DCN changes in cerebellar degeneration. These changes mediate virtually all cerebellar outflows along with the vestibular nuclei. Quantitative assessment of the DCN may be invaluable to diagnosis, staging, and prognosis in neurodegenerative diseases with cerebellar involvement. DTI evaluation of the DCN can serve as a simple imaging biomarker of cerebellar disease [7–10]. Sajjadi et al. showed that neurodegenerative disease is identifiable in a single subject with DTI [11]. Neuroimaging evidence of microstructural changes consistent with neurodegeneration has been found in patients with familial essential tremor [12].

DTI reveals disease-specific DCN changes in cerebellar degeneration. The method used in this study should be applied to SCA3 and Friedreich’s ataxia, which may show significant dentate involvement. Based on the aforementioned studies, it is important to use DTI for quantifying the microstructural damage to white matter in neurodegenerative diseases caused by SCA12 [13–16].

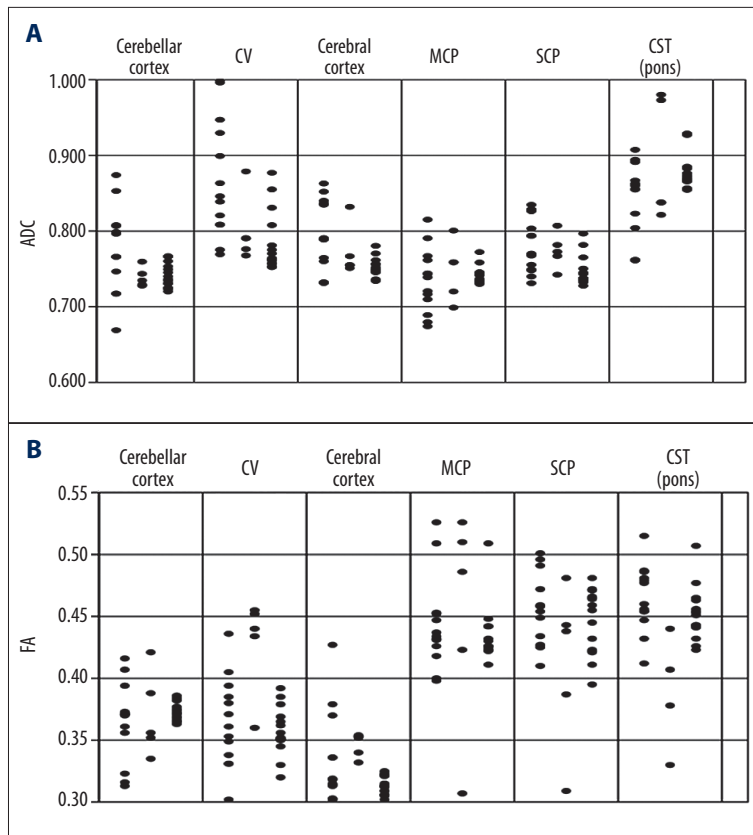


Figure 2. DTI imaging results.

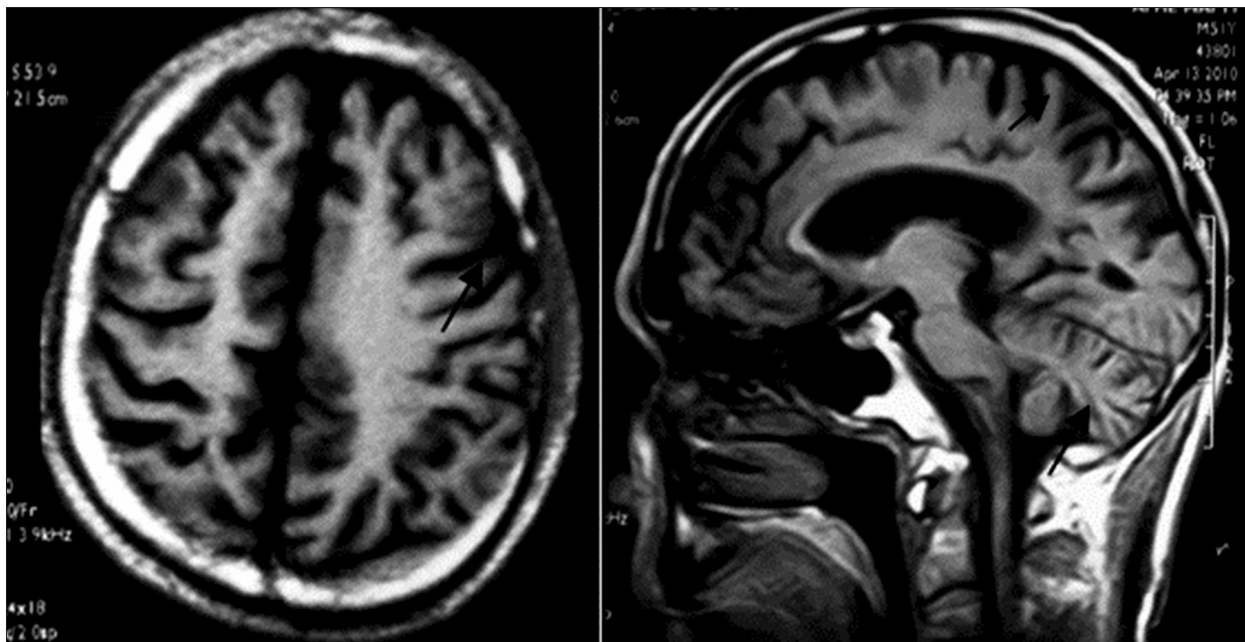


Figure 3. Scatterplot of ADC (A) and FA (B) measurements. For each ROI, the columns are presented in the following order: patients with SCA12, presymptomatic patients with SCA12, and controls.

The detection of SCA12 subtypes of microstructural damage in cerebral white matter using DTI has not been reported in detail. O'Hearn et al. reported that no focal signal abnormalities

in grey or white matter have been reported in SCA12 brain images. In the present study, some differences in ADC values in the CV of the patients and presymptomatic patients [6,17]

were found. Moreover, the presymptomatic patients and control group exhibited differences in the positions of the CeC and CC. FA values of the presymptomatic patients and control group decreased in the CV region, which may indicate the onset of symptoms in patients with pre-existing microstructural damage in cerebral white matter of the CV [17–19]. Thus, the detection of DTI changes in the assessment of the structural damage in white matter of the CV may be used as relatively objective morphological markers to assess the outcome in presymptomatic patients.

Mandelli et al. [19] reported that DTI does not differ between SCA1 and SCA2. However, strongly significant differences were found between the 2 subtypes compared with the controls, and correlations with clinical scores were detected. Compared with the controls, ADC significantly increased in the MCP and hemispheric white matter in SCA1, and in all regions under consideration in SCA2. Reports on other subtypes of white matter damage using DTI detection are rare [20–23].

The results in our study show that the course of the disease and ADC values of CV were highly positively correlated ($r=0.71$). SARA score and ADC values of CV also showed a highly positive correlation ($r=0.72$). Damage in the brain white matter fiber structure of the CV could reflect the severity of damage of SCA12 nerve pathology. This finding was consistent with the report of O'Hearn et al., who found that the CV appears more atrophic than the cerebellar hemispheres. Thus, our results suggest that neurodegenerative pathology of CeC and CV white matter structures may have a key function in disease onset.

Further studies are necessary to assess the function of FA and mean diffusivity changes in the differential diagnosis of SCA12, which may present similar clinical signs at disease onset. Although the degree of atrophy was not measured quantitatively, visual assessment performed in clinical practice was determined to be adequate for the purpose of the present study. Although a certain margin for rating subjectivity remained, blinding prevented bias [24–26].

References:

1. Srivastava AK, Choudhry S, Gopinath MS et al: Molecular and clinical correlation in five Indian families with spinocerebellar ataxia 12. *Ann Neurol*, 2001; 50: 796–800
2. Bahl S, Virdi K, Mittal U et al: Evidence of a common founder for SCA12 in the Indian population. *Ann Hum Genet*, 2005; 69: 528–34
3. Dagda RK, Merrill RA, Cribbs JT et al: The spinocerebellar ataxia 12 gene product and protein phosphatase 2A regulatory subunit Bbeta2 antagonizes neuronal survival by promoting mitochondrial fission. *J Biol Chem*, 2008; 283: 36241–48
4. Holmes SE, O'Hearn EE, McInnis MG et al: Expansion of a novel CAG trinucleotide repeat in the 5' region of PPP2R2B is associated with SCA 12. *Nat Genet*, 1999; 23: 391–92
5. O'Hearn E, Holmes SE, Calvert PC et al: SCA-12: tremor with cerebellar and cortical atrophy is associated with a CAG repeat expansion. *Neurology*, 2001; 56: 299–303
6. O'Hearn E, Holmes SE, Margolis RL: Spinocerebellar ataxia type 12. *Handb Clin Neurol*, 2012; 103: 535–47
7. Della Nave R, Foresti S, Tessa C et al: ADC mapping of neurodegeneration in the brainstem and cerebellum of patients with progressive ataxias. *Neuroimage*, 2004; 22: 698–705
8. Du AX, Cuzzocreo JL, Landman BA et al: Diffusion tensor imaging reveals disease-specific deep cerebellar nuclear changes in cerebellar degeneration. *J Neurol*, 2010; 257: 1406–8
9. Matilla-Dueñas A, Ashizawa T, Brice A et al: Consensus paper: pathological mechanisms underlying neurodegeneration in spinocerebellar ataxias. *Cerebellum*, 2014; 13: 269–302

Diffusion tensor tractography is an excellent tool for imaging individual white matter tracts. However, the technical limitations of this method should be considered, particularly problems concerning fiber crossing, delineation of tracts using manually drawn ROIs, and distortion of axonal and neuronal architecture in neurodegenerative diseases; these limitations make it difficult for the tracking algorithm to follow the fibers over longer distances or changes in direction [19,27,28].

Conclusions

DTI is useful in differentiating patients with SCA12, but has limitations when used in the presymptomatic patients and controls because of the substantial overlap among the 3 groups. The strongly significant differences and correlations with clinical scores suggest an important function in combination with structural imaging characterizing the phenotypes, and provide a quantitative measure of disease severity.

Data

Data from a single Uyghur pedigree were collected, among which 13 cases were patients and 54 cases were “healthy” individuals from Xinjiang.

Acknowledgements

This work was supported by grants from the Autonomous Region Nature Foundation 2011211A063. The authors thank the patients and their family members who participated in the investigations of SCA12. We also thank Hong Jiang, Yunling Wang, Jingxu Ma, Tao Liu, and Shutao Zheng (Xinjiang Medical University) for technical assistance.

Conflict of interest

On behalf of all authors, the corresponding author states that there is no conflict of interest.

10. Schmitz-Hübsch T, du Montcel ST, Baliko L et al: Scale for the assessment and rating of ataxia: development of a new clinical scale. *Neurology*, 2006; 66: 1717–20
11. Sajjadi SA, Acosta-Cabrero J, Patterson K et al: Diffusion tensor magnetic resonance imaging for single subject diagnosis in neurodegenerative diseases. *Brain*, 2013; 136: 2253–61
12. Nicoletti G, Manners D, Novellino F et al: Diffusion tensor MRI changes in cerebellar structures of patients with familial essential tremor. *Neurology*, 2010; 74: 988–94
13. Guerrini L, Lolli F, Ginestroni A et al: Brainstem neurodegeneration correlates with clinical dysfunction in SCA1 but not in SCA2. A quantitative volumetric, diffusion and proton spectroscopy MR study. *Brain*, 2004; 127: 1785–95
14. Kelp A, Koeppen AH, Petrasch-Parwez E et al: A novel transgenic rat model for spinocerebellar ataxia type 17 recapitulates neuropathological changes and supplies *in vivo* imaging biomarkers. *J Neurosci*, 2013; 33: 9068–81
15. Prakash N, Hageman N, Hua X et al: Patterns of fractional anisotropy changes in white matter of cerebellar peduncles distinguish spinocerebellar ataxia-1 from multiple system atrophy and other ataxia syndromes. *Neuroimage*, 2009; 47: 1772–81
16. Reimão S, Morgado C, Neto L et al: Diffusion Tensor Imaging in Movement Disorders: Review of Major Patterns and Correlation with Normal Brainstem/cerebellar White Matter. *Neuroradiol J*, 2011; 24: 177–86
17. Solodkin A, Peri E, Chen EE et al: Loss of intrinsic organization of cerebellar networks in spinocerebellar ataxia type 1: correlates with disease severity and duration. *Cerebellum*, 2011; 10: 218–32
18. Guimarães RP, D'Abreu A, Yasuda CL: A multimodal evaluation of microstructural white matter damage in spinocerebellar ataxia type 3. *Mov Disord*, 2013; 28: 1125–32
19. Mandelli ML, De Simone T, Minati L et al: Diffusion tensor imaging of spinocerebellar ataxias types 1 and 2. *Am J Neuroradiol*, 2007; 28: 1996–2000
20. Della Nave R, Ginestroni A, Tessa C et al: Brain white matter damage in SCA1 and SCA2. An *in vivo* study using voxel-based morphometry, histogram analysis of mean diffusivity and tract-based spatial statistics. *Neuroimage*, 2008; 43: 10–19
21. Duffy SL, Paradise M, Hickie IB et al: Cognitive impairment with and without depression history: an analysis of white matter microstructure. *J Psychiatry Neurosci*, 2014; 39: 135–43
22. Novak MJ, Seunarine KK, Gibbard CR et al: White matter integrity in pre-manifest and early Huntington's disease is related to caudate loss and disease progression. *Cortex*, 2014; 52: 98–112
23. Zhu T, Hu R, Tian W et al: SPatial REgression Analysis of Diffusion tensor imaging (SPREAD) for longitudinal progression of neurodegenerative disease in individual subjects. *Magn Reson Imaging*, 2013; 31: 1657–67
24. Müller HP, Kassubek J: Diffusion tensor magnetic resonance imaging in the analysis of neurodegenerative diseases. *J Vis Exp*, 2013; 28: e50427
25. Van Camp N, Blockx I, Camón L et al: A complementary diffusion tensor imaging (DTI)-histological study in a model of Huntington's disease. *Neurobiol Aging*, 2012; 33: 945–59
26. Wang PS, Wu HM, Lin CP, Soong BW: Use of diffusion tensor imaging to identify similarities and differences between cerebellar and Parkinsonism forms of multiple system atrophy. *Neuroradiology*, 2011; 53: 471–81
27. Bohanna I, Georgiou-Karistianis N, Sritharan A et al: Diffusion tensor imaging in Huntington's disease reveals distinct patterns of white matter degeneration associated with motor and cognitive deficits. *Brain Imaging Behav*, 2011; 5: 171–80
28. Rosas HD, Tuch DS, Hevelone ND et al: Diffusion tensor imaging in presymptomatic and early Huntington's disease: Selective white matter pathology and its relationship to clinical measures. *Mov Disord*, 2006; 21: 1317–25